New Structural Model for the Si(331)-(12 × 1) Surface Reconstruction

Corsin Battaglia,[1] Katalin Gaál-Nagy,[2] Claude Monney,[1] Clément Didiot,[1] Eike Fabian Schwier,[1] Michael Gunnar Garnier,[1] Giovanni Onida,[2] and Philipp Aebi[1]

[1]*Institut de Physique, Université de Neuchâtel, 2000 Neuchâtel, Switzerland*

[2]*Dipartimento di Fisica and European Theoretical Spectroscopy Facility (ETSF), Università di Milano, 20133 Milano, Italy*

(Received 24 July 2008; published 9 February 2009)

A new structural model for the Si(331)-(12 × 1) surface reconstruction is proposed. Based on scanning tunneling microscopy images of unprecedented resolution, low-energy electron diffraction data, and first-principles total-energy calculations, we demonstrate that the reconstructed Si(331) surface shares the same elementary building blocks as the Si(110)-(16 × 2) surface, establishing the pentamer as a universal building block for complex silicon surface reconstructions.

DOI: 10.1103/PhysRevLett.102.066102 PACS numbers: 68.35.bg, 61.05.jh, 68.37.Ef, 71.15.Mb

The study of semiconductor surface reconstructions has been an area of active research for many years and has gained tremendous importance with the advent of low-dimensional heteroepitaxial semiconductor nanostructures such as quantum dots and quantum wires [1]. The creation of a surface results in broken bonds, called dangling bonds. Dangling bonds are energetically unfavorable causing surface atoms to rearrange or reconstruct. This often results in highly complex atomic structures, whose determination remains a formidable challenge and requires the complementary role of different experimental and theoretical methods. In order to lower the surface energy, silicon surfaces adopt a variety of strategies allowing to reduce the number of dangling bonds. Despite the large number of known surface reconstructions, one frequently encounters common elementary structural building blocks [2,3]. Identifying these building blocks is important not only for a better understanding of these surfaces, but also serves as a guide for the elaboration of new structural models.

Two of the most important strategies, encountered for instance on Si(100) [4] and Si(111) [5], are, respectively, the formation of dimers, where two surface atoms pair up to eliminate their dangling bonds, and the appearance of adatoms, which bond to three surface atoms thus saturating three dangling bonds. An important step towards the understanding of high-index group IV surfaces with a surface normal in between the (111) and (100) direction was the introduction of an additional reconstruction element by Dabrowski *et al.* [6]. They proposed a sixfold coordinated surface self-interstitial which is captured by a conglomerate of surface atoms [7,8]. This concept was subsequently adapted by An [9] and theoretically analyzed by Stekolnikov [10,11] to explain the pairs of pentagons observed in scanning tunneling microscopy (STM) images of the reconstructed Si(110) surface.

In this Letter we focus on the atomic structure of the Si(331)-(12 × 1) reconstruction. We present high-resolution STM images resolving for the first time rows of pentagons very similar to the ones observed on Si(110)-(16 × 2). Si(331), whose surface normal is located 22.0° away from the (111) direction towards (110) [see Fig. 1(a)], is an important surface, since it is the only confirmed planar silicon surface with a stable reconstruction located between (111) and (110). Since the discovery of the Si(331)-(12 × 1) reconstruction more than 17 years ago [12] several structural models containing dimers and adatoms have been proposed [13,14]. However, none of these models is able to explain the pentagons observed in our STM images. Combining the complementary strength of STM, low-energy electron diffraction (LEED), and first-

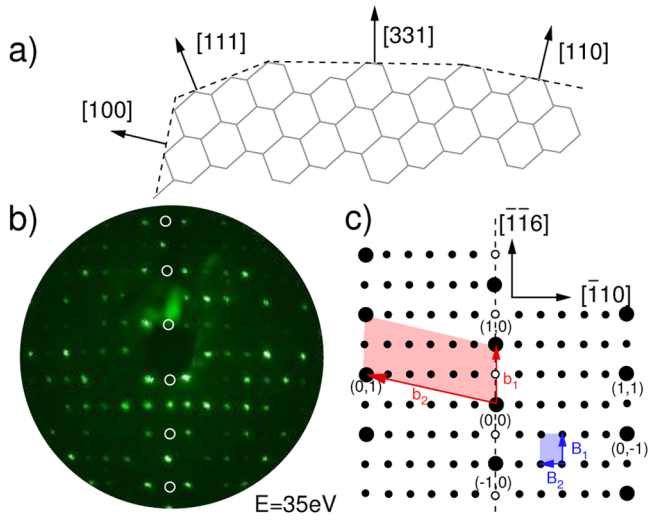

FIG. 1 (color online). (a) Side cutaway showing the crystal lattice of silicon in the ($\bar{1}$10) plane. The dashed line follows the bulk-terminated surface for several important orientations. (b) Experimental LEED pattern at 35 eV beam energy. The positions of missing spots are indicated by the white circles. (c) Sketch of the LEED pattern with (1 × 1) and (12 × 1) reciprocal unit cells and spot labels (black). The bulk directions are also given. The positions of the missing spots are indicated by empty black circles. The orientation of the glide plane is indicated by a dashed line.

 © 2009 The American Physical Society

principles total-energy calculations, we derive a new structural model containing surface self-interstitials as basic building blocks.

Experiments were carried out in an ultrahigh vacuum chamber with a residual gas pressure below 3×10^{-11} mbar equipped with an Omicron LT-STM and Omicron Spectaleed LEED/Auger optics. Sample preparation is described in detail in Ref. [15]. The theoretical results are based on first-principles calculations within density functional theory (DFT) performed with ABINIT [16], which was already successfully applied to describe the Si(113) surface [17]. Details on the calculations will be published in Ref. [18].

Figure 1(b) presents a normal incidence LEED pattern of the Si(331)-(12 × 1) reconstruction. The corresponding sketch containing reciprocal lattice vectors and spot labels (h, k) is shown in Fig. 1(c). The bulk-terminated surface is chosen as the reference for indexing. The reciprocal unit cell vectors $\mathbf{B}_1$ and $\mathbf{B}_2$ of the reconstructed surface can be expressed using the reciprocal unit cell vectors $\mathbf{b}_1$ and $\mathbf{b}_2$ of the bulk-terminated (331) surface

$$\begin{pmatrix} \mathbf{b}_1 \\ \mathbf{b}_2 \end{pmatrix} = \begin{pmatrix} 2 & 0 \\ 1 & 6 \end{pmatrix} \begin{pmatrix} \mathbf{B}_1 \\ \mathbf{B}_2 \end{pmatrix}.$$

However, since in general we find 11 satellite diffraction spots in between the integer spots along the $[\bar{1}10]$ direction, the reconstruction is conventionally called the (12 × 1) reconstruction in the literature.

The spot intensities in the LEED pattern in Fig. 1(b) exhibit a mirror symmetry along the $[\bar{1}\,\bar{1}\,6]$ direction. Furthermore, a careful analysis of the LEED spot intensities as a function of energy (not shown) reveals that systematically all half-order spots $(\pm nh/2, 0)$, n being an odd integer, are missing for all beam energies [see empty circles in Figs. 1(b) and 1(c)]. Although spot intensities vary as a function of energy and even vanish at some energies due to diffraction effects, the $(\pm nh/2, 0)$ spots exhibit no intensity at all beam energies. Such missing spots indicate the existence of a glide plane along $[\bar{1}\,\bar{1}\,6]$ in real space [19,20]. This glide plane also implies the mirror symmetry observed for the LEED intensities in reciprocal space [21]. Thus LEED firmly establishes the presence of a glide plane in the structure.

We now turn to our STM data. The large scale topography image presented in Fig. 2(a) shows the high quality of the surface. Besides the perfect long range order only a few local defects are present on the surface. As already observed by several other groups [14,22–26], the Si(331)-(12 × 1) reconstruction consists of similar mounds arranged into zigzag chains running along the $[\bar{1}\,\bar{1}\,6]$ direction separated by trenches. Focusing now on the high-resolution image in Fig. 2(b) we see that each of the mounds consists of five protrusions forming a pentagon. A further protrusion may be identified linking two successive pentagons within the same chain. Pentagons

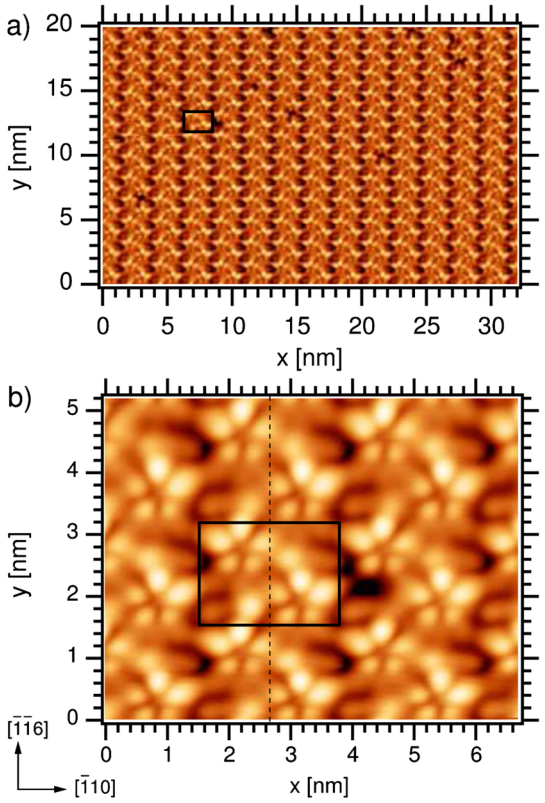

FIG. 2 (color online). (a) Large scale STM topography of the annealed Si(331) surface. (b) High-resolution image with unit cell (full line) and the glide plane (dashed line) indicated. Bias voltage 2.0 V, set-point current 0.06 nA, temperature 77 K.

with the same dimensions were already observed on Ge(110)-c(8 × 10) [27,28] as well as on Ge(110)-(16 × 2) [27] and on Si(110)-(16 × 2) [9]. To our knowledge this is the first observation of such pentagons on a surface away from the (110) orientation, indicating their high stability and confirming their fundamental role as an elementary building block in semiconductor surface reconstructions.

Inspired by structural elements encountered on reconstructed Si(113) and Ge(113) surfaces [6,7], An *et al.* [9] have proposed an adatom-tetramer-interstitial (ATI) model for the pentagons observed on the (110) surfaces. Its stability has subsequently been tested theoretically by means of first-principles total-energy calculations [10,11].

In the following, we develop a coherent structural model for the Si(331)-(12 × 1) reconstruction inspired by the ATI model and discuss similarities and differences with the (110) case. In a first step we need to determine the registry of the surface reconstruction with respect to the bulk. This is not a trivial task, so we proceed in two steps. We focus first on the position of the surface reconstruction with respect to the underlying bulk along the $[\bar{1}10]$ direction. Here the occurrence of the glide plane symmetry gives us the clue. Inspection of Fig. 2(b) shows that a glide plane is found at the center of the zigzag chain (dashed line) consistent with the observation of missing spots in the LEED pattern. The glide plane found on the surface must also be a

glide plane of the bulk, since the space group of the bulk contains all symmetry elements of the surface. A side view of the bulk-terminated Si(331) surface is shown in Fig. 3(a) with a top view of our model in Fig. 3(b). The dashed line represents the glide plane. Figure 3(c) offers a graphical proof for the existence of the glide plane in the bulk. After mirror reflection along the glide plane line, a translation by half the unit vector $-\mathbf{A}_1/2$ is necessary to obtain the original registry.

After determining the registry of the surface reconstruction with respect to the $[\bar{1}10]$ direction we now need to study the registry with respect to the $[\bar{1}\,\bar{1}\,6]$ direction. Here we benefit from a comparison with the Si(110) surface shown schematically in Figs. 3(e) and 3(f). For a sketch of the complete model for the Si(110)-(16 × 2) reconstruction including the steps along $[\bar{1}12]$ see Ref. [11]. According to the ATI model for the Si(110) surface, the pentagon seen in STM images consists of four adatoms (*a*, *b*, *c*, *d*, empty circles) forming the tetramer and one surface atom (*e*, black dot) belonging to the first atomic layer [see Fig. 3(d)]. The sixfold coordinated interstitial atom (*f*, empty circle) is located at the center of the pentagon slightly below the tetramer plane and consequently not directly visible in STM images (see simulated STM images in Ref. [11]). The resulting structural element formed by the tetramer, atom *e* and *f* combined is called a pentamer [11].

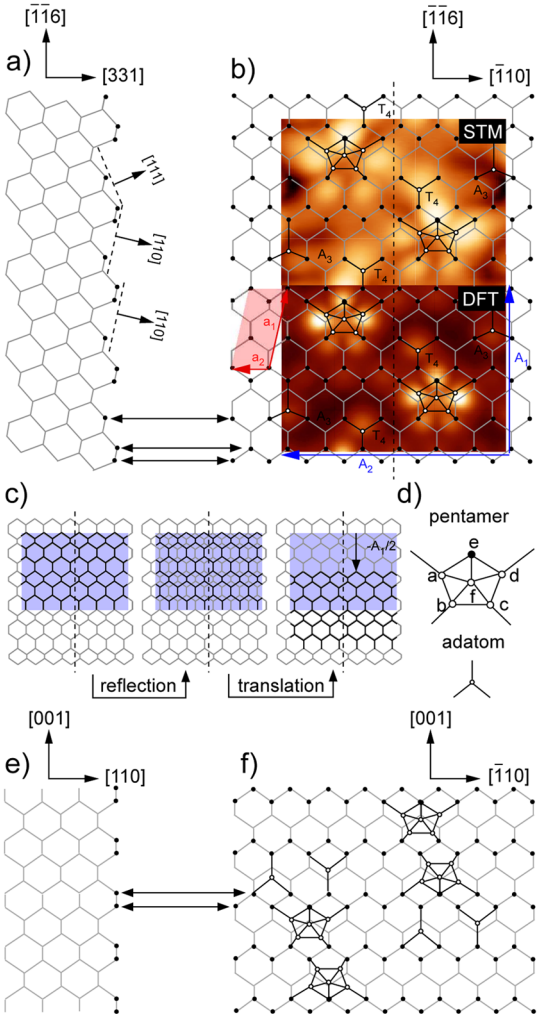

FIG. 3 (color online). (a) Side and (b) top view of the Si(331) surface. Black dots indicate the position of surface atoms carrying a dangling bond, some of which are saturated by pentamers and adatoms (empty circles). Surface atoms whose dangling bond is not saturated are rest atoms. The (1 × 1) and (12 × 1) unit cells are shown. For comparison an experimental and a simulated STM image is underlaid. The dashed line represents the glide plane. (c) Graphical proof for the existence of the glide plane. (d) Sketch of the pentamer and the adatom with atom labels. (e) Side and (f) top view of the Si(110) surface (see text).

In order to integrate the pentamer building block into our model we note that the arrangement of dangling bonds on the bulk-truncated surface represented by black dots and marked by the double headed arrows in Fig. 3 differs between the Si(110) and Si(331) surface. Whereas dangling bonds on the Si(110) surface occur in double rows running along $[\bar{1}10]$, double rows alternate with single rows of dangling bonds on the bulk-terminated Si(331) surface. For the Si(110) structure, atom *e* actually belongs to one of these dangling bond double rows. Consequently we also anchor the two pentamers per unit cell required by STM on the double dangling bond row of the bulk-terminated Si(331) surface. It is important to note that anchoring the pentamers in this way provides exactly the same local binding configuration as on the Si(110) surface, since careful comparison of the sideviews in Figs. 3(a) and 3(e) reveals that the bulk-truncated Si(331) surface can be viewed as a highly stepped Si(110) surface. The selected position of the pentagons agrees with the position observed in the STM images [see STM image behind the model in Fig. 3(b)]. Note also that the single dangling bond row of the Si(331) surface is slightly lower-lying than the double dangling bond row, causing an inclination of the pentamer, in agreement with the lower intensity of the lobes associated with adatom *b* and *c* in the experimental STM image.

Each pentamer saturates five of the surrounding dangling bonds [10]. By introducing two pentamers per Si(331)-(12 × 1) unit cell, the number of dangling bonds has been reduced from 36 to 26. Some of the remaining dangling bonds are saturated by simple adatoms as in the case of the Si(110) surface. In the STM image in Fig. 2(b) the additional protrusion linking two successive pentamers indicates the location of a first adatom, labeled T_4 in Fig. 3(b) in analogy with the convention used to label this adatom position on the (111) surface. The local binding configuration for this T_4 adatom on the Si(331) surface is exactly the same as on the (111) surface, where adatoms are common structural building blocks. A further adatom labeled A_3 saturates three more dangling bonds.

Introducing two T_4 and two A_3 adatoms per unit cell into our structural model further reduces the number of dangling bonds from 26 to 14. For Si(110) Stekolnikov *et al.* [11] have noted that it is energetically more favorable to

leave some surface atoms, so-called rest atoms, unsaturated than to introduce the maximum number of adatoms into the model, since this allows a further reduction of the surface energy by electron transfer from the adatom to the rest atom in analogy with the Si(111)-(7×7) case [29].

We have explicitly verified the stability of the reconstruction containing two T_4 and two A_3 adatoms by means of first-principles calculations testing various alternative adatom configurations, among which the present one yields the highest stability (details on the theoretical calculation including a ball-and-stick representation of our relaxed model will be published elsewhere [18]). The addition of two pentamers per unit cell reduces the surface energy by 12.2 ± 0.3 meV/Å^2 with respect to the bulk-truncated surface. The energy is further lowered by 7.1 ± 0.3 meV/Å^2 when adding two T_4 and two A_3 adatoms. However, some of the investigated adatom configurations are found to lie very close in energy, with the lowest energy configuration being favored by at least 1.7 ± 0.3 meV/Å^2.

In Fig. 3(b) we also show a simulated STM image based on relaxed coordinates of our structural model, obtained by integrating the local state density over a 2.0 eV energy window corresponding to the experimental STM bias voltage. The DFT image is in excellent agreement with the experimental STM image. The theoretical image reproduces well the strong intensity of the lobes associated with atoms *a*, *e* and *d* and the weaker intensity associated with atoms *b* and *c* of the pentamer. In general the topographical features in the simulated image show better resolution and less diffuse character than the corresponding features observed in STM, since the simulation neglects any role of the tip structure in degrading image resolution [30]. In the experimental as well as in the simulated image, individual pentagons do not exhibit a mirror symmetry along the $[\bar{1}\,\bar{1}\,6]$ direction indicating a distortion of the pentagon which allows to reduce internal strain. Furthermore the T_4 and A_3 adatoms in the simulated image are seen as a marked protrusion in agreement with experiment.

In summary, by combining STM, LEED, first-principles calculations and by comparing similarities and differences between the Si(331)-(12×1) and Si(110)-(16×2) reconstructions, we have derived a complete structural model for the Si(331) surface containing the pentamer as an essential ingredient. Thus besides adatoms, dimers and tetramers, pentamers emerge as a universal building blocks for silicon surface reconstructions.

Stimulating discussions with Antje Schmalstieg, Georg Held, Pascal Ruffieux, and Oliver Gröning are gratefully acknowledged. Skillfull technical assistance was provided by our workshop and electric engineering team. This work was supported by the Fonds National Suisse pour la Recherche Scientifique through Div. II and the Swiss National Center of Competence in Research MaNEP. We acknowledge support by the European Community through the ''Nanoquanta NoE'' and ''ETSF-I3'' projects (NMP4-CT-2004-500198 and Grant Agreement No. 211956) for the theoretical results, which are an outcome of the ETSF User Project No. 94.

[1] F. M. Ross, R. M. Tromp, and M. C. Reuter, Science **286**, 1931 (1999).
[2] C. Battaglia, K. Gaál-Nagy, C. Monney, C. Didiot, E. F. Schwier, M. G. Garnier, G. Onida, and P. Aebi, J. Phys. Condens. Matter **21**, 013001 (2009).
[3] C. Battaglia, H. Cercellier, C. Monney, M. G. Garnier, and P. Aebi, Europhys. Lett. **77**, 36003 (2007).
[4] D. J. Chadi, Phys. Rev. Lett. **43**, 43 (1979).
[5] K. Takayanagi, Y. Tanishiro, M. Takahashi, and S. Takahashi, J. Vac. Sci. Technol. A **3**, 1502 (1985).
[6] J. Dabrowski, H.-J. Müssig, and G. Wolff, Phys. Rev. Lett. **73**, 1660 (1994).
[7] A. Laracuente, S. C. Erwin, and L. J. Whitman, Phys. Rev. Lett. **81**, 5177 (1998).
[8] A. A. Stekolnikov, J. Furthmüller, and F. Bechstedt, Phys. Rev. B **67**, 195332 (2003).
[9] T. An, M. Yoshimura, I. Ono, and K. Ueda, Phys. Rev. B **61**, 3006 (2000).
[10] A. A. Stekolnikov, J. Furthmüller, and F. Bechstedt, Phys. Rev. B **70**, 045305 (2004).
[11] A. A. Stekolnikov, J. Furthmüller, and F. Bechstedt, Phys. Rev. Lett. **93**, 136104 (2004).
[12] J. Wei, E. D. Williams, and R. L. Park, Surf. Sci. Lett. **250**, L368 (1991).
[13] B. Z. Olshanetsky, S. A. Teys, and I. G. Kozhemyako, Phys. Low-Dim. Struct. **11/12**, 85 (1998).
[14] Z. Gai, R. G. Zhao, T. Sakurai, and W. S. Yang, Phys. Rev. B **63**, 085301 (2001).
[15] C. Battaglia, C. Monney, C. Didiot, E. F. Schwier, M. Mariotti, M. G. Garnier, and P. Aebi, arXiv:0809.4967.
[16] http://www.abinit.org.
[17] K. Gaál-Nagy and G. Onida, Phys. Rev. B **75**, 155331 (2007).
[18] C. Battaglia, K. Gaál-Nagy, G. Onida, and P. Aebi (to be published).
[19] B. W. Holland and D. P. Woodruff, Surf. Sci. **36**, 488 (1973).
[20] W. S. Yang and F. Jona, Phys. Rev. B **29**, 899 (1984).
[21] M. K. Debe and D. A. King, Phys. Rev. Lett. **39**, 708 (1977).
[22] H. Tanaka, Y. Watanabe, and I. Sumita, Appl. Surf. Sci. **60**, 474 (1992).
[23] H. Hibino, T. Fukuda, M. Suzuki, Y. Homma, T. Sato, M. Iwatsuki, K. Miki, and H. Tokumoto, Phys. Rev. B **47**, 13027 (1993).
[24] H. Tanaka, T. Yokoyama, and I. Sumita, Appl. Surf. Sci. **76–77**, 340 (1994).
[25] H. Hibino and T. Ogino, Surf. Sci. **357–358**, 102 (1996).
[26] H. Hibino and T. Ogino, Phys. Rev. B **53**, 15682 (1996).
[27] T. Ichikawa, T. Sueyosi, T. Saot, M. Iwatsuki, F. Udagwa, and I. Sumita, Solid State Commun. **93**, 541 (1995).
[28] Z. Gai, R. G. Zhao, and W. S. Yang, Phys. Rev. B **57**, R6795 (1998).
[29] R. D. Meade and D. Vanderbilt, Phys. Rev. B **40**, 3905 (1989).
[30] A. A. Baski, S. C. Erwin, and L. J. Whitman, Science **269**, 1556 (1995).